AD-A066 059 AIR FORCE WEAPONS LAB KIRTLAND AFB N MEX F/G 20/11
SAP IV ANALYSIS OF A REENTERING MULTI-HUNDRED WATT HEAT SOURCE --ETC(U)
SEP 78 M L CRAWFORD

UNCLASSIFIED AFWL-TR-78-95 SBIE-AD-E200 243 NL

| OF |
AD
A066058

END
DATE
FILMED
5-79
DDC

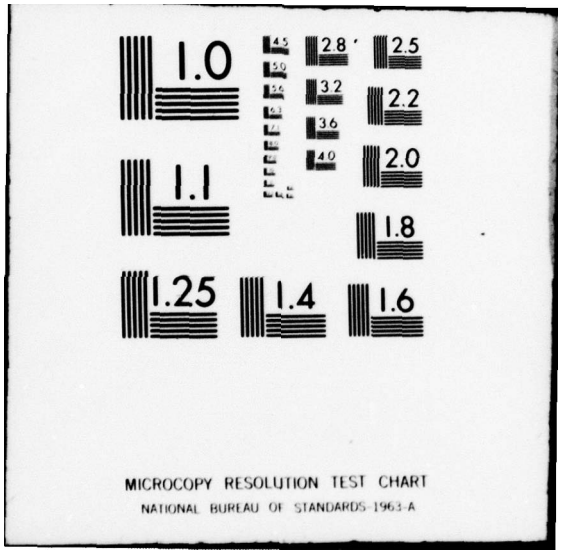
1.0
1.1
1.25
1.4
1.6
1.8
2.0
2.2
2.5
2.8
3.2
3.6
4.0
4.5
5.0
MICROCOPY RESOLUTION TEST CHART
NATIONAL BUREAU OF STANDARDS-1963-A

AFWL-TR-78-95

(2) LEVEL II

AFWL-TR-78-95

SAP IV ANALYSIS OF A REENTERING MULTI-HUNDRED WATT HEAT SOURCE ASSEMBLY

Michael L. Crawford, Lt, USAF

September 1978

Final Report

AIR FORCE WEAPONS LABORATORY
Air Force Systems Command
Kirtland Air Force Base, NM 87117

This final report was prepared by the Air Force Weapons Laboratory, Kirtland Air Force Base, New Mexico under Job Order 20070318. Lt Michael L. Crawford (DYV) was the Laboratory Project Officer-in-Charge.

When US drawings, specifications, or other data are used for any purpose other than a definitely related Government procurement operation, the Government thereby incurs no responsibility nor any obligation whatsoever, and the fact that the Government may have formulated, furnished, or in any way supplied the said drawings, specifications, or other data is not to be regarded by implication or otherwise as in any manner licensing the holder or any other person or corporation or conveying any rights or permission to manufacture, use, or sell any patented invention that may in any way be related thereto.

This report has been reviewed by the Information Office (OI) and is releasable to the National Technical Information Service (NTIS). At NTIS, it will be available to the general public, including foreign nations.

This technical report has been reviewed and is approved for publication.

Michael L. Crawford

MICHAEL L. CRAWFORD
Lt, USAF
Project Officer

FOR THE COMMANDER

George L Williams

GEORGE L. WILLIAMS
Major, USAF
Chief, Environment and Effects Branch

Thomas W Ciambrone

THOMAS W. CIAMBRONE
Lt Colonel, USAF
Chief, Applied Physics Division

DO NOT RETURN THIS COPY. RETAIN OR DESTROY.

UNCLASSIFIED

SECURITY CLASSIFICATION OF THIS PAGE (When Data Entered)

REPORT DOCUMENTATION PAGE

READ INSTRUCTIONS BEFORE COMPLETING FORM

(14) 1. REPORT NUMBER: AFWL-TR-78-95

2. GOVT ACCESSION NO.

3. RECIPIENT'S CATALOG NUMBER

(6) 4. TITLE (and Subtitle): SAP IV ANALYSIS OF A REENTERING MULTI-HUNDRED WATT HEAT SOURCE ASSEMBLY.

(9) 5. TYPE OF REPORT & PERIOD COVERED: Final Report.

6. PERFORMING ORG. REPORT NUMBER

(10) 7. AUTHOR(s): Michael L. Crawford

8. CONTRACT OR GRANT NUMBER(s)

9. PERFORMING ORGANIZATION NAME AND ADDRESS
Air Force Weapons Laboratory (DYV)
Kirtland Air Force Base, NM 87117

10. PROGRAM ELEMENT, PROJECT, TASK AREA & WORK UNIT NUMBERS
62601F
(16) 20070318
(17) 03

11. CONTROLLING OFFICE NAME AND ADDRESS
Air Force Weapons Laboratory (DYV)
Kirtland Air Force Base, NM 87117

(11) 12. REPORT DATE: September 1978

13. NUMBER OF PAGES: 25

14. MONITORING AGENCY NAME & ADDRESS (if different from Controlling Office)

(12) 29 p.

15. SECURITY CLASS. (of this report): UNCLASSIFIED

15a. DECLASSIFICATION/DOWNGRADING SCHEDULE

16. DISTRIBUTION STATEMENT (of this Report)

Approved for public release; distribution unlimited.

17. DISTRIBUTION STATEMENT (of the abstract entered in Block 20, if different from Report)

(18) SBIE (19) AD-E200 243

18. SUPPLEMENTARY NOTES

19. KEY WORDS (Continue on reverse side if necessary and identify by block number)

Radioisotopic Thermoelectric Generators
Structural Analysis
Finite Element Computer Codes

20. ABSTRACT (Continue on reverse side if necessary and identify by block number)

The results of a three-dimensional stress analysis of a reentering Multi-Hundred Watt Heat Source Assembly are presented. The SAP IV computer program was used for a static analysis of the aeroshell for the maximum stress reentry hypothesized for the NASA Voyager launches. The temperature profile through the aeroshell thickness was applied with given external aerodynamic and inertial loads, and because the axial thermal gradients are unknown at the point of maximum combined stress, a longitudinal temperature gradient which is present (over)

→ next page

DD FORM 1 JAN 73 1473 EDITION OF 1 NOV 65 IS OBSOLETE

UNCLASSIFIED

SECURITY CLASSIFICATION OF THIS PAGE (When Data Entered)

013 150

at 0.4 seconds later in the reentry is used. Therefore, the results can only be used for "order-of-magnitude" estimates of the increase in calculated stress, and they indicate an increase on the order of 10 percent over previous SAP IV calculations.

CONTENTS

ILLUSTRATIONS

SECTION I

INTRODUCTION

The Multi-Hundred Watt Radioisotopic Thermoelectric Generator (MHW-RTG) is used as the power generation system for the NASA Voyager 1977 spacecraft. The use of plutonium fuel in these RTGs necessitated an extensive nuclear safety evaluation and risk assessment of the Voyager launches. This safety evaluation consisted primarily of a review of the RTG contractor's Final Safety Analysis Report (FSAR) (ref. 1) and preparation of a Safety Evaluation Report (SER) by the Interagency Nuclear Safety Review Panel (INSRP). One area of concern which received a great deal of attention during the safety review was the possibility of an accidental reentry of the spacecraft into the earth's atmosphere.

The total reentry analysis was a complex task, involving several organizations. The General Dynamics/Convair Division calculated the initial vehicle velocity and entry angle (V-γ) conditions (ref. 2). From this V-γ map, four reentry conditions were selected for detailed analysis: shallow, maximum stress, orbital decay, and powered reentry. The Jet Propulsion Laboratory studied spacecraft breakup and determined the conditions at the time of RTG release for each of these reentry conditions (ref. 1, Appendix B). The General Electric Space Division (the RTG contractor) analyzed the RTG and Heat Source Assembly (HSA) thermal responses, the release of the HSA, and the aeroshell and ablation sleeve stresses (ref. 1, Appendix E). It was found that the maximum stresses in the aeroshell occurred for a V-γ of 36,000 fps and -46° (at 400,000 ft) and at 12.9 s after reentry (defined as 400,000 ft).

If the maximum allowable stress was exceeded, the aeroshell would fail causing release of the internal Fuel Sphere Assemblies (FSAs); therefore, a thorough stress analysis of the reentering HSA was required. The preliminary

---

1. Final Safety Analysis Report for the MJS-77 Mission, Doc. No. 77SDS4206, General Electric Company, Space Division, Philadelphia, PA, January 1977.

2. MJS '77 RTG Safety Study - Phase II. Range Safety Equipment, Launch Pad Hazards, Launch Vehicle Failure Probabilities and Reentry Environment, Doc. No. CASD/LVP 76-004, General Dynamics Convair Division, San Diego, CA, 7 July 1975.

analysis involved a plane stress approximation for the aeroshell and ablation sleeve center sections using the GE ORTHOSAFE computer program. This approximation neglected axial stresses, so the second technique modified the plane stress analysis for three-dimensional effects by applying a longitudinal stress distribution to maintain a plane aeroshell cross section. The final analysis was a three-dimensional stress calculation using the SAP IV computer program. This analysis used an R-Θ temperature profile, but assumed the temperature was constant along the aeroshell length. (For a detailed discussion of the stress analyses, see reference 1, Appendix E.)

The results of these three analyses are shown in Table 1. The maximum allowable aeroshell stress was 7214 psi, and therefore it was not predicted to fail; i.e., a positive margin of safety was calculated.

Table 1

RESULTS OF THE AEROSHELL STRESS ANALYSIS

	Plane Stress	3-D Modification	SAP IV
Maximum Calculated Stress	6050	6949	6186

The plane stress, three-dimensional modification, and SAP IV calculations described above neglected the effect of a three-dimensional temperature field. This report investigates this effect, specifically on the SAP IV results. Since the longitudinal temperature variations are not known at 12.9 s after reentry, the precise effect on the stress magnitudes and distributions cannot be determined; however, the three-dimensional temperatures are known at 13.3 s after reentry. Combining the temperatures at these two different times during the reentry would, of course, be meaningless. But if the temperature gradients along the aeroshell length are on the same order of magnitude for the two slightly different times, then an estimate of the change in predicted aeroshell stress at 12.9 s due to three-dimensional temperatures can be calculated by applying the 13.3 s longitudinal temperature gradients. The results of the SAP IV calculations presented below are therefore hypothetical axial temperature gradients, and can only be used for order-of-magnitude estimates.

A brief description of the input mesh and boundary conditions, material properties, temperature profiles, and external loadings will be made (largely taken directly from the FSAR), followed by a presentation of the SAP IV results and the conclusions.

SECTION II

THREE-DIMENSIONAL FINITE ELEMENT MESH

A schematic diagram of the three-dimensional mesh used as input to the SAP-IV program is shown in figure 1. This mesh is identical to that used in the FSAR. It contains 1776 elements and 2475 node points.

Boundary Conditions: Due to symmetry, only one-quarter of the aeroshell was modeled. The nodes lying in the X-Y centerplane were restrained in the Z-direction, and the nodes lying in the X-Z centerplane were restrained in the Y-direction. The third boundary condition was artificially introduced to simulate the effect of the endcap.

Although the aeroshell endcap was not modeled in this analysis, its contribution in maintaining the shape of the end of the aeroshell was simulated. This rigidity effect was modeled by applying an internal load at the lock-ring groove. This load was varied in the X-Y plane (or R-Θ direction), and its profile was opposite in direction to that of the opposing aerodynamic load (see Section V). A scaling factor was applied to the internal load and this factor was adjusted to restrict movement. (Since a costly and time-consuming iteration technique was used, exact counterbalancing of the loads was impractical. The iterations were therefore terminated when the change in aeroshell stresses was less than 1 percent.)

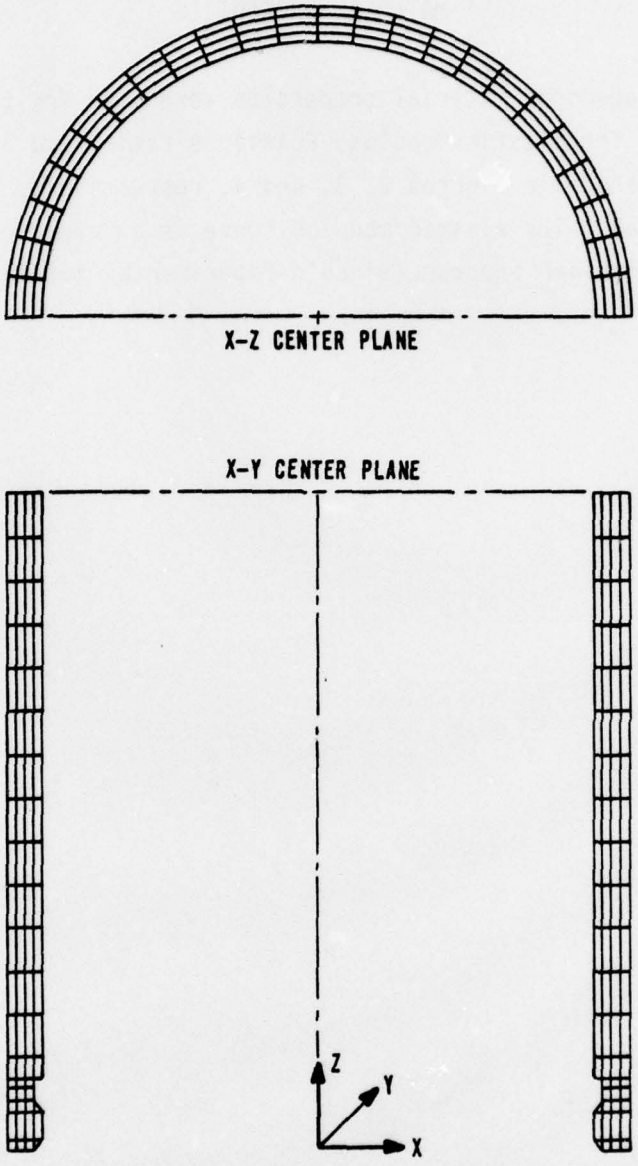

Figure 1. Finite Element Mesh Used for the SAP IV Analysis

SECTION III

MATERIAL PROPERTIES

Temperature dependent material properties were used for the aeroshell POCO graphite AXF-5Q. The elastic modulus, Poisson's ratio, and linear coefficient of expansion are shown in figures 2, 3, and 4, respectively. These curves were taken from the FSAR. The elastic modulus curve is an average based on the data obtained from an earlier program (Lincoln Experimental Satellites 8 and 9 aeroshell).

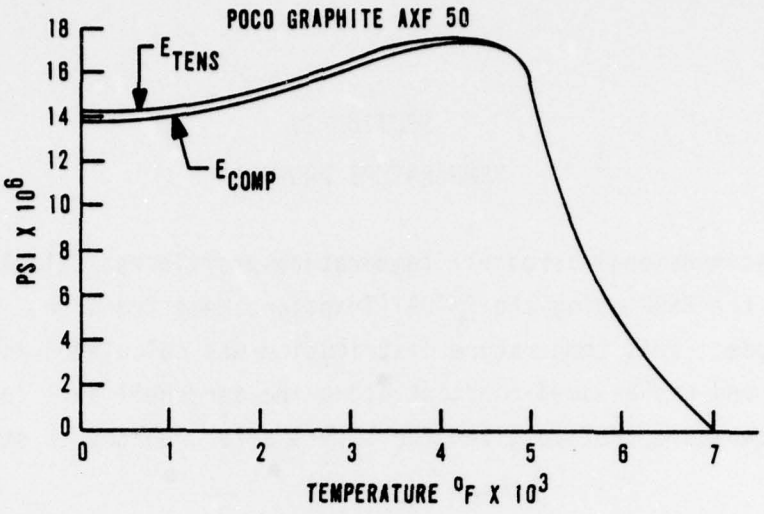

Figure 2. Initial Elastic Modules vs Temperature

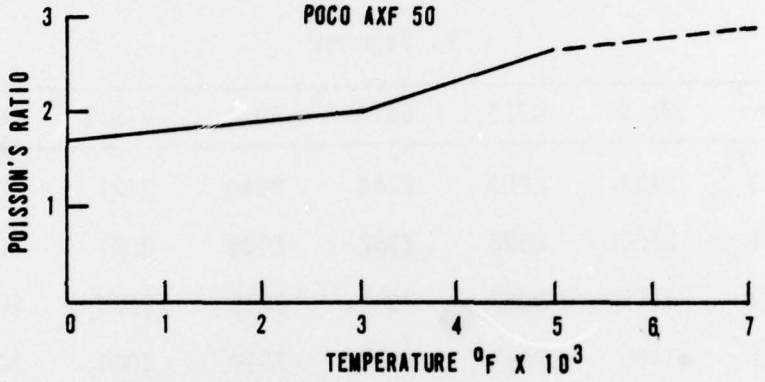

Figure 3. Poisson's Ratio vs Temperature

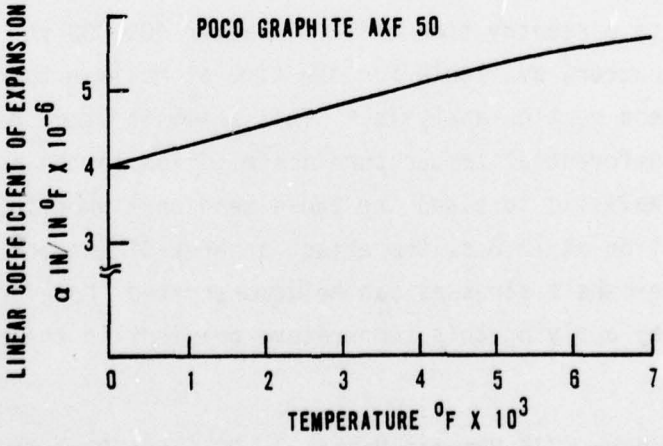

Figure 4. Linear Coefficient of Expansion versus Temperature

SECTION IV
TEMPERATURE PROFILES

The two-dimensional aeroshell temperature profile was calculated and reported in the FSAR using the THTDA (Transient Heat Transfer - Version D - Ablation) code. This temperature distribution was calculated for R-θ spacial dependence, and was assumed constant along the aeroshell axis (or Z-direction). The R-θ temperature profile given for 12.9 s after reentry is shown in Table 2

Table 2

AEROSHELL TEMPERATURE MATRIX (Reference 1)

	θ, Degrees							
R, in.	0.0	21.0	42.5	66.4	90.0	118.6	151.5	18.0
3.280	2243	2433	2380	2244	2040	2021	2013	2006
3.410	2584	2663	2596	2382	2105	2027	2015	2010
3.535	3109	3117	3057	2681	2218	2045	2026	2021
3.595	3463	3450	3442	2937	2314	2064	2038	2033

The three-dimensional aeroshell temperature distribution was not calculated for the time after reentry for maximum combined stress (thermal plus aerodynamic), which corresponds to a reentry time of 12.9 s after 400,000 ft. The axial distribution is, however, available for the time at maximum thermal stress (13.3 s) from the end section analysis.* This analysis used the THTDA code to calculate the circumferential temperature distribution in the aeroshell endcap. Although it is unrealistic to blend the two-dimensional profile at 12.9 s with the axial distribution at 13.3 s, the effect a three-dimensional temperature field has on the aeroshell stresses can be demonstrated (however, only quantitatively estimated) by applying this temperature gradient in the axial direction.

*Letter from G. Drenker (MJS Program Manager), GE Space Division, to C. P. Melfi, Aerospace Corporation, El Segundo, CA, 10 March 1977.

The axial temperature gradients are plotted in figures 5 through 8. The indicated gradients were applied to the temperature profiles in Table 2 beginning at 2.5 in from the end of the aeroshell. From the centerplane to 2.5 from the end, the temperature was assumed constant in the axial (Z) direction.

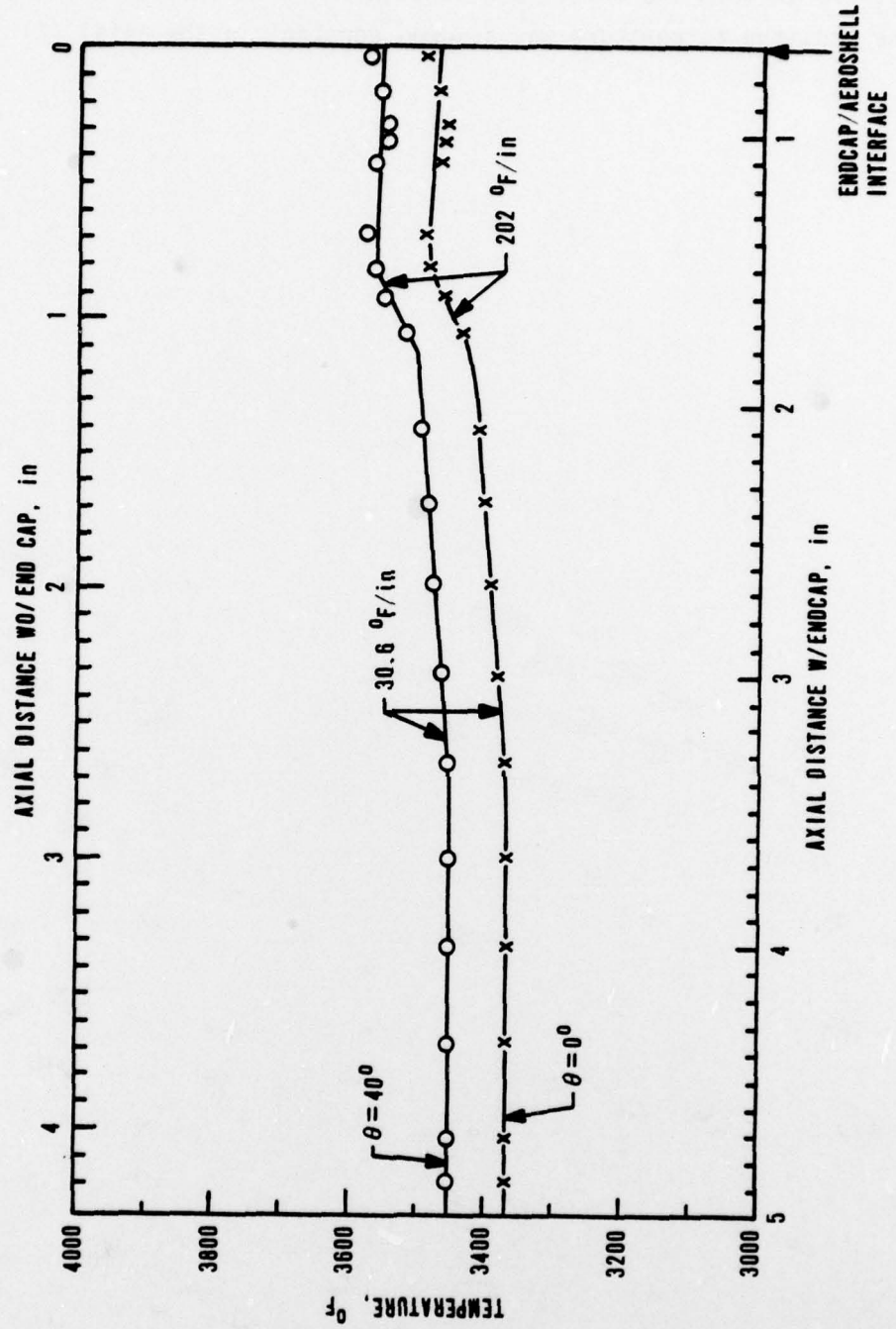

Figure 5. Axial Temperature Distribution at a Radius of 3.558 in at 13.3 s after 400 kft

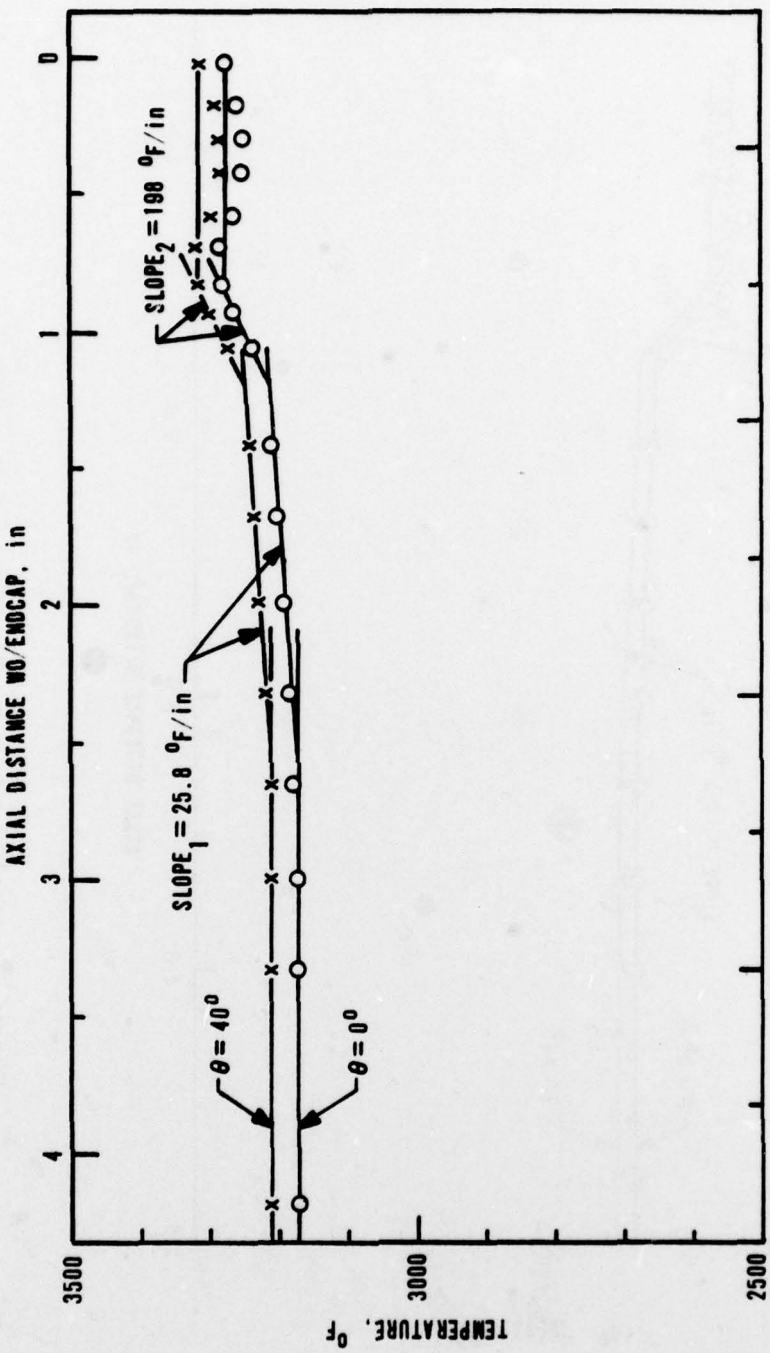

Figure 6. Axial Temperature Distribution at a Radius of 3.520 in at 13.3 s after 400 kft

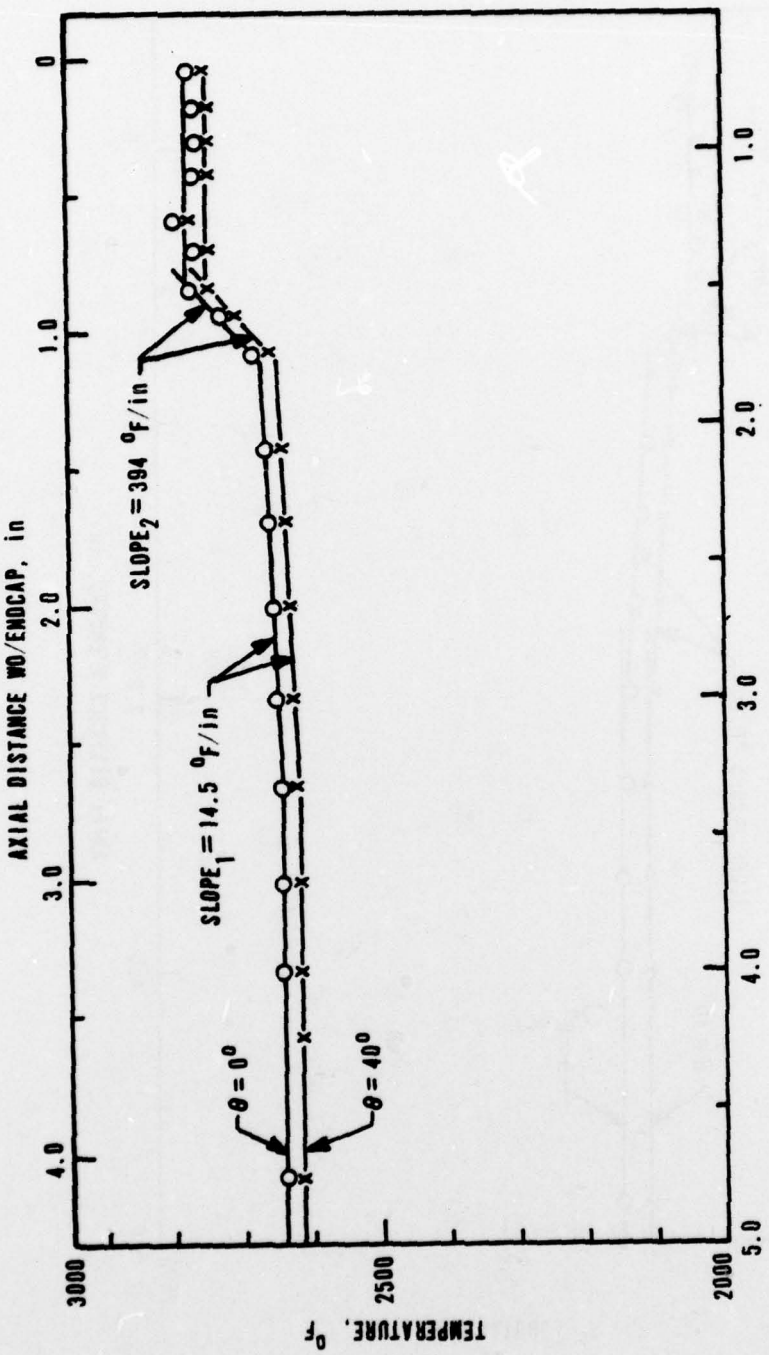

Figure 7. Axial Temperature Distribution at a Radius of 3.370 in at 13.3 s after 400 kft

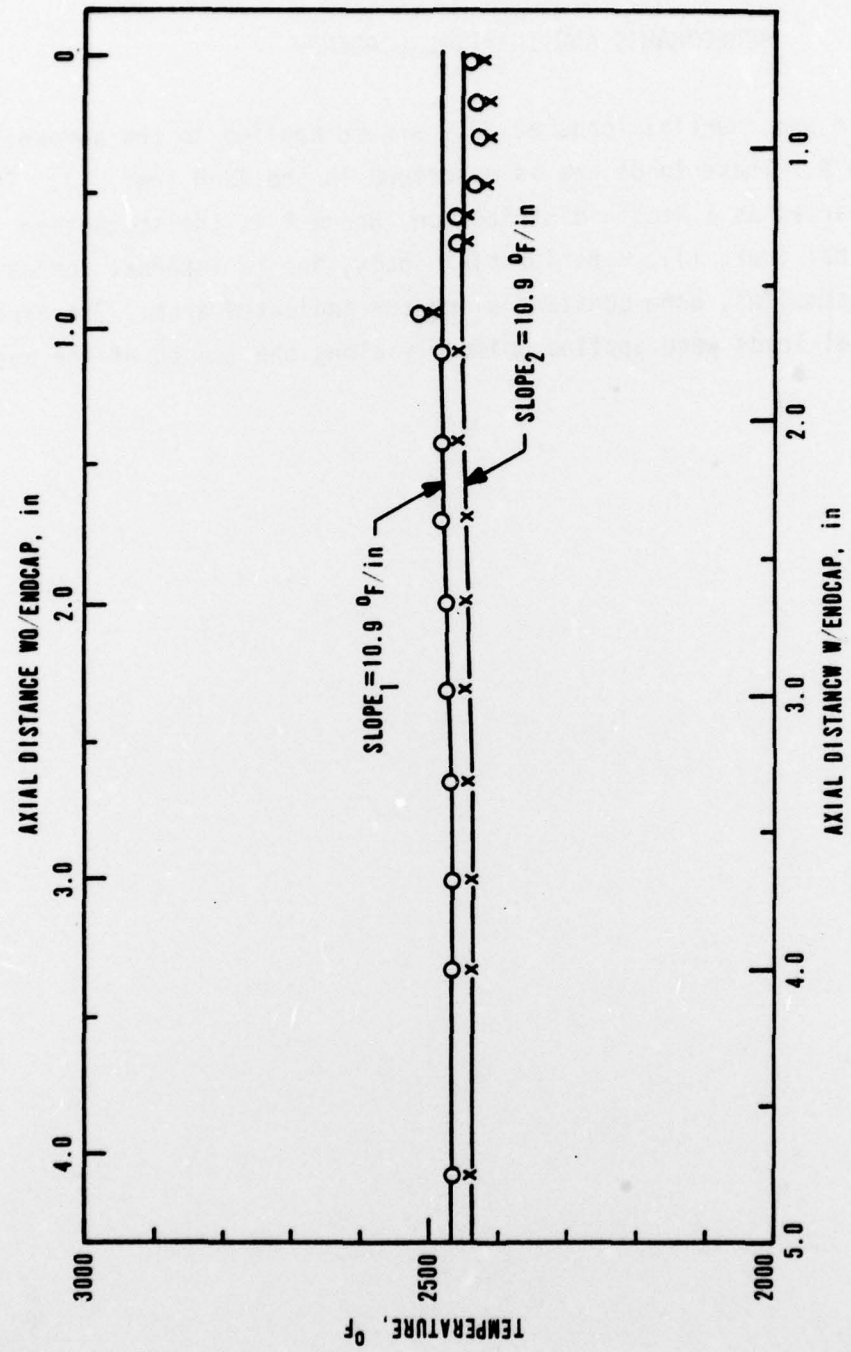

Figure 8. Axial Temperature Distribution at a Radius of 3.260 in at 13.3 s after 400 kft

SECTION V

AERODYNAMIC AND INERTIAL LOADING

The aerodynamic and inertial loads at 12.9 s were applied to the aeroshell as shown in figure 9. These loads are as described in the FSAR (ref. 1). The aerodynamic load varied as a $P\cos^2\alpha$ distribution, where P is the stagnation pressure (P = 118 psi (ref. 1)). The inertial loads, due to internal forces of the fuel sphere assemblies, were constant along the indicated arcs. The aerodynamic and inertial loads were applied uniformly along the length of the aeroshell.

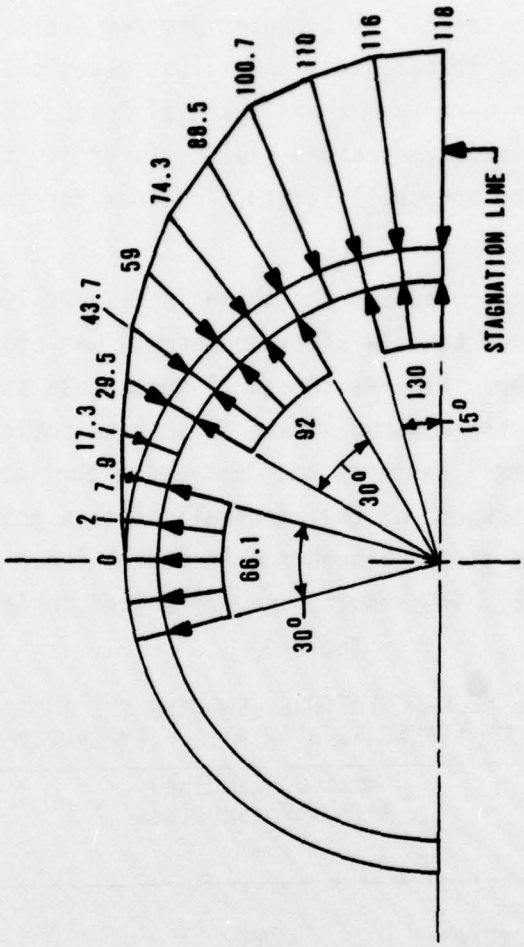

Figure 9. Externally Applied Aerodynamic and Inertial Loads, Assumed Constant Along the Aeroshell Length

SECTION VI

RESULTS

The mesh, material properties, temperature fields, and external loads described above were input to the SAP IV computer program (refs. 3 and 4). The code was run for two cases, to calculate thermal stresses only and then to calculate thermal stress plus aerodynamic and inertial loads. These two calculations were made for each of the two temperature fields, first for the case of a constant temperature along the aeroshell length, and then for the case of an axial temperature gradient.

The results of these calculations are shown in figures 10 through 15. The critical area, where maximum tensile stress occurred, was along the stagnation line at the inside diameter. Figures 10 and 11 show these stress profiles. Along the inner diameter, the maximum stress is seen to occur at an area 6.25 to 6.50 in from the aeroshell centerplane, just above the lock-ring groove. The stress through the thickness of the aeroshell at this point is shown in figures 12 and 13, and the stress around the aeroshell inner circumference is shown in figures 14 and 15. The results are summarized in Table 3.

Table 3

RESULTS OF THE CALCULATIONS, SHOWING THE INCREASE IN MAXIMUM STRESS WITH AN AXIAL TEMPERATURE

	Maximum Combined Principle Stresses KSI	Percent Increase
Constant Axial Temperatures	7066	10.8
Axial Temperature Gradients	7828	

3. Bathe, K. J.; E. L. Wilson; F. E. Peterson; SAP IV - A Structural Analysis Program for Static and Dynamic Response of Linear Systems, EERC 73-11 University of California, Earthquake Engineering Research Center, Berkeley, CA, June 1973.

4. Melfi, C. P.; J. L. Johnson; Viking and LES 8/9 Reentry Nuclear Safety Studies, Volume II, Supplementary Reentry Response Analysis, AFWL-TR-76-164 Vol II, Air Force Weapons Laboratory, Kirtland Air Force Base, NM, September 1976.

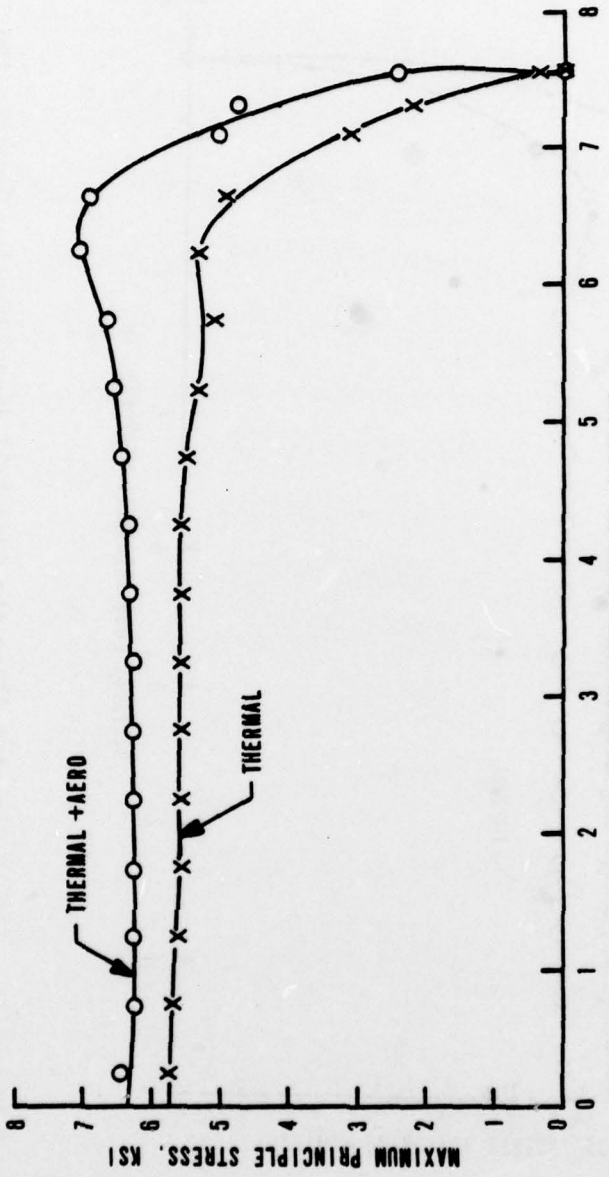

Figure 10. SAP IV Stresses Along the Aeroshell Inner Diameter Opposite the Stagnation Line for the Constant Axial Temperatures

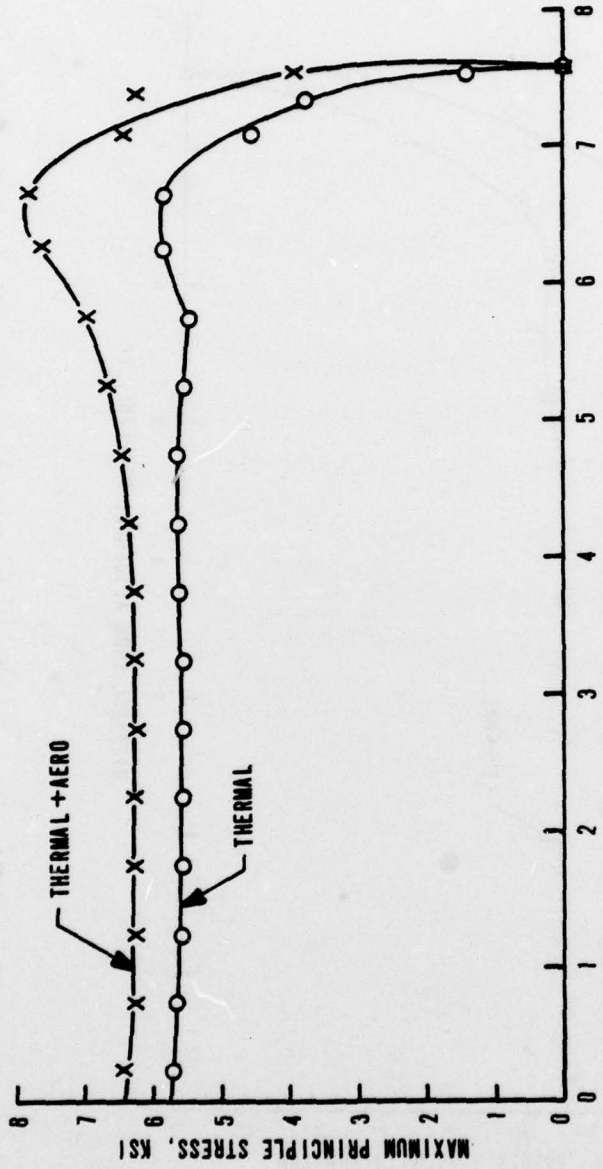

Figure 11. SAP IV Stresses Along the Aeroshell Inner Diameter Opposite the Stagnation Line for the Applied Gradients to the Axial Temperatures

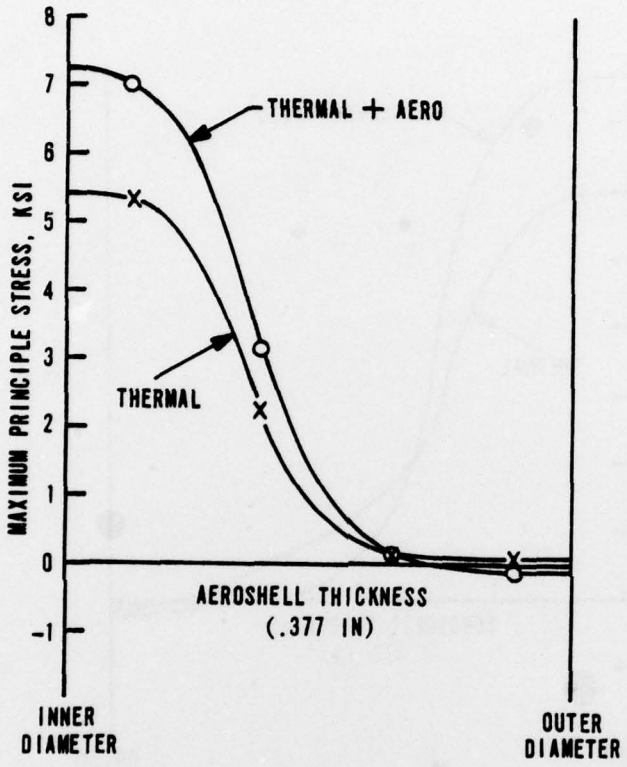

Figure 12. Stress Profile Through the Aeroshell Thickness at the Stagnation Line for the Constant Axial Temperatures

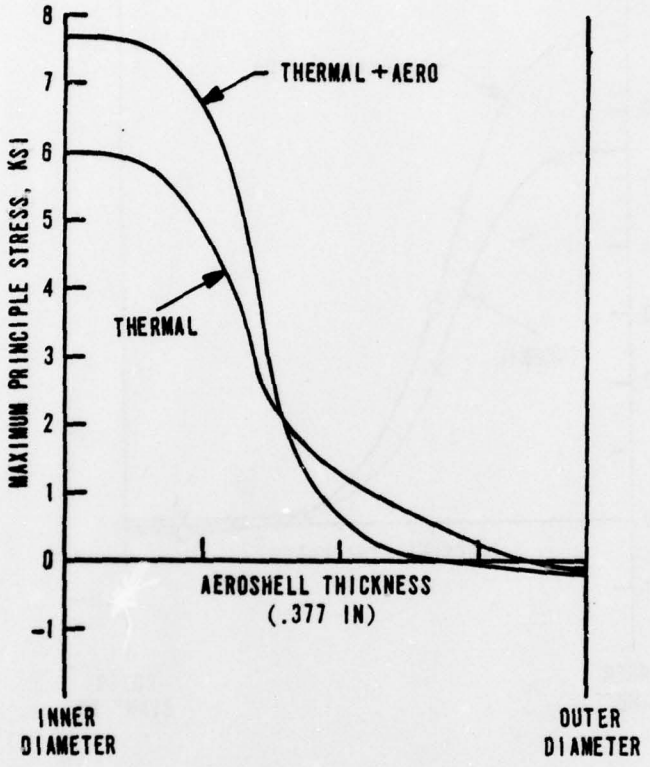

Figure 13. Stress Profile Through the Aeroshell Thickness at the Stagnation Line for the Applied Gradients to the Axial Temperatures

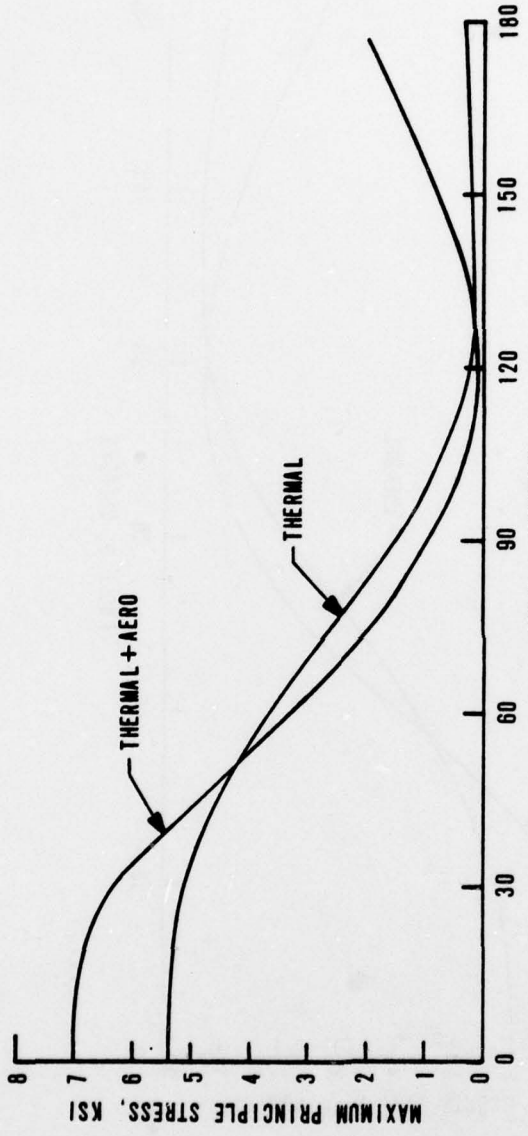

Figure 14. Stress Distribution Around the Aeroshell Inner Diameter at the Midplane for the Constant Axial Temperatures

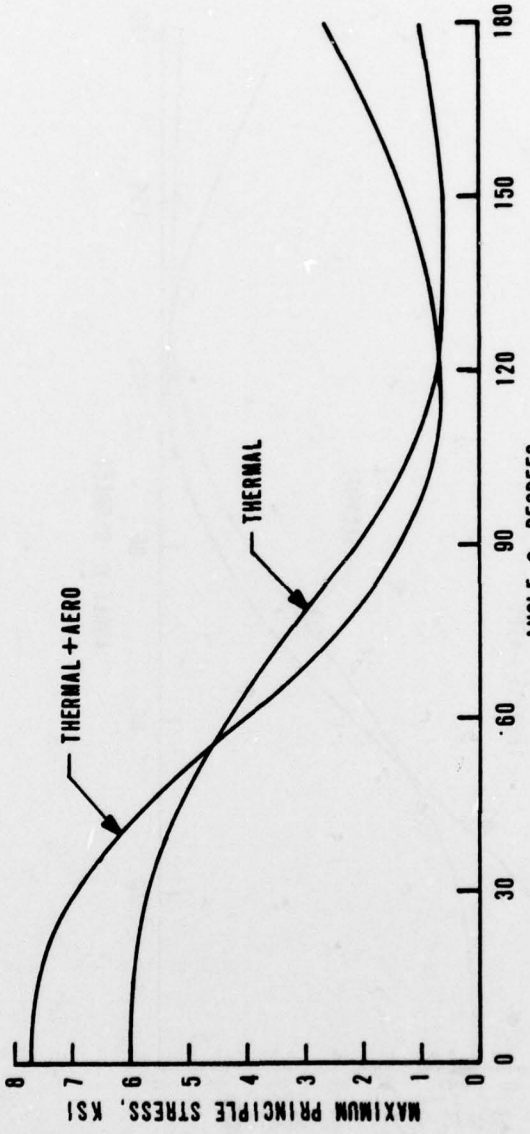

Figure 15. Stress Distribution Around the Aeroshell Inner Diameter at the Midplane for the Applied Gradients to the Axial Temperatures

SECTION VII

CONCLUSIONS

This report has demonstrated the increase in calculated stresses when a longitudinal gradient is applied to an R-θ temperature field. The results indicate an increase in calculated stress when an axial temperature gradient is applied, and if the magnitudes of the gradients at 12.9 and 13.3 s after reentry are similar, an increase of approximately 10 percent is indicated. Reference 5 describes an alternative, probabilistic (error analysis) approach which may be useful in the risk assessment for accident analyses which indicate decreasing margins of safety.

5. Anderson, D. C., et al., Voyager - Analysis and Risk Assessment, AFWL-TR-77-161, Air Force Weapons Laboratory, Kirtland Air Force Base, NM, published June 1978.